Bimodal behavior and isobestic transition pathway in surface plasmon resonance sensing

Anuj Dhawan, Michael Canva, Tuan Vo-Dinh

Bimodal behavior and isobestic transition pathway in surface plasmon resonance sensing

Anuj Dhawan,[1,2,4,*] Michael Canva,[4,5] and Tuan Vo-Dinh[2,3,4]

[1]*Department of Electrical Engineering, Indian Institute of Technology-Delhi, New Delhi 110016, India*
[2]*Department of Biomedical Engineering, Duke University, Durham, North Carolina 27708, USA*
[3]*Department of Chemistry, Duke University, Durham, North Carolina 27708, USA*
[4]*Fitzpatrick Institute for Photonics, Duke University, Durham, North Carolina 27708, USA*
[5]*Laboratoire Charles Fabry, Institut d'Optique Graduate School, Univ Paris Sud, CNRS, Campus Polytechnique 91127 Palaiseau cedex, France*
**adhawan@ee.iitd.ac.in*

Abstract: In traditional interpretation of surface plasmon resonance (SPR) sensing and imaging data, total surface coverage of adsorbed or deposited chemical and biological molecules is generally assumed. This homogenous assumption leads to the modeling of monomodal propagation of plasmons on the surface of the metallic film corresponding to a certain relative permittivity and thickness of the medium—such as molecular thin film—next to the metal. In actual SPR Imaging (SPRI) and SPR sensing situations, the plasmonics-active platforms (e.g., biochips) employed may capture the biomolecular targets as aggregates of different domain sizes on the surface of the thin metallic films. Indeed, such binding of target material always has a finite thickness and is characterized by aggregate lateral sizes possibly varying from tens of nanometers to hundreds of micrometers. This paper studies the propagation of surface plasmons in metallic films, with dielectric domain sizes varying within such ranges. Through rigorous coupled wave analysis (RCWA) calculations, it is indicated that when the domain size is small, only a single mode of propagation—i.e. 'monomodal' propagation behavior—occurs as indicated by only one dip in the angular reflectance curves associated with metallic film having a periodically structured array of molecules on its surface. On the other hand, as the domain size is increased, there is a transition from the 'monomodal propagation behavior' to the existence of a 'mixture of monomodal and bimodal propagation behavior', which changes to a purely 'bimodal behavior' after the size of the domain periodicity is increased beyond about ten micron. Such a transition pathway clearly exhibits isobestic points. The calculations presented in this paper can enable correct interpretation of experimental angular or spectral reflectance data.

OCIS codes: (240.6680) Surface plasmons; (050.1755) Computational electromagnetic methods; (260.2110) Electromagnetic optics; (260.3910) Metal optics; (160.4236) Nanomaterials; (280.4788) Optical sensing and sensors.

References and links

1. H. Raether, *Surface Plasmons on Smooth and Rough Surfaces and on Gratings* (Springer-Verlag, 1988)
2. E. Kretschmann, "Determination of optical constants of metals by excitation of surface plasmons," Z. Phys. **241**(4), 313–324 (1971).
3. J. Homola, *Surface Plasmon Resonance Based Sensors* (Springer, 2006).
4. M. Malmqvist, "Surface plasmon resonance for detection and measurement of antibody-antigen affinity and kinetics," Curr. Opin. Immunol. **5**(2), 282–286 (1993).
5. P. Schuck, "Use of surface plasmon resonance to probe the equilibrium and dynamic aspects of interactions between biological macromolecules," Annu. Rev. Biophys. Biomol. Struct. **26**(1), 541–566 (1997).
6. R. Slavík, J. Homola, J. Čtyroký, and E. Brynda, "Novel spectral fiber optic sensor based on surface plasmon resonance," Sens. Actuators B Chem. **74**(1-3), 106–111 (2001).

#165623 - $15.00 USD Received 2 Apr 2012; revised 16 May 2012; accepted 14 Jun 2012; published 1 Oct 2012

7. R. C. Jorgenson and S. S. Yee, "A fiber optic chemical sensor based on surface plasmon resonance," Sens. Actuators B Chem. **12**(3), 213–220 (1993).
8. U. Schröter and D. Heitmann, "Grating couplers for surface plasmons excited on thin metal films in the Kretschmann-Raether configuration," Phys. Rev. B **60**(7), 4992–4999 (1999).
9. A. G. Brolo, R. Gordon, B. Leathem, and K. L. Kavanagh, "Surface plasmon sensor based on the enhanced light transmission through arrays of nanoholes in gold films," Langmuir **20**(12), 4813–4815 (2004).
10. A. Degiron and T. W. Ebbesen, "The role of localized surface plasmon modes in the enhanced transmission of periodic subwavelength apertures," J. Opt. A, Pure Appl. Opt. **7**(2), S90–S96 (2005).
11. H. J. Lezec and T. Thio, "Diffracted evanescent wave model for enhanced and suppressed optical transmission through subwavelength hole arrays," Opt. Express **12**(16), 3629–3651 (2004).
12. F. Bardin, A. Bellemain, G. Roger, and M. Canva, "Surface plasmon resonance spectro-imaging sensor for biomolecular surface interaction characterization," Biosens. Bioelectron. **24**(7), 2100–2105 (2009).
13. J. Hottin, J. Moreau, G. Roger, J. Spadavecchia, M. C. Millot, M. Goossens, and M. Canva, "Plasmonic DNA: towards genetic diagnosis chips," Plasmonics **2**(4), 201–215 (2007).
14. P. Lisboa, A. Valsesia, I. Mannelli, S. Mornet, P. Colpo, and F. Rossi, "Sensitivity enhancement of surface-plasmon resonance imaging by nanoarrayed organothiols," Adv. Mater. (Deerfield Beach Fla.) **20**(12), 2352–2358 (2008).
15. M. Nakkach, A. Duval, B. Ea-Kim, J. Moreau, and M. Canva, "Angulo-spectral surface plasmon resonance imaging of nanofabricated grating surfaces," Opt. Lett. **35**(13), 2209–2211 (2010).
16. P. Lecaruyer, E. Maillart, M. Canva, and J. Rolland, "Generalization of the Rouard method to an absorbing thin-film stack and application to surface plasmon resonance," Appl. Opt. **45**(33), 8419–8423 (2006).
17. M. G. Moharam and T. K. Gaylord, "Rigorous coupled-wave analysis of metallic surface-relief gratings," J. Opt. Soc. Am. A **3**(11), 1780–1787 (1986).
18. A. Dhawan, S. J. Norton, M. D. Gerhold, and T. Vo-Dinh, "Comparison of FDTD numerical computations and analytical multipole expansion method for plasmonics-active nanosphere dimers," Opt. Express **17**(12), 9688–9703 (2009).
19. A. Dhawan, A. Duval, M. Nakkach, G. Barbillon, J. Moreau, M. Canva, and T. Vo-Dinh, "Deep UV nano-micro-structuring of substrates for surface plasmon resonance imaging," Nanotechnology **22**(16), 165301 (2011).
20. A. Dhawan, M. Canva, and T. Vo-Dinh, "Narrow groove plasmonic nano-gratings for surface plasmon resonance sensing," Opt. Express **19**(2), 787–813 (2011).
21. W. L. Barnes, "Surface plasmon–polariton length scales: a route to sub-wavelength optics," J. Opt. A, Pure Appl. Opt. **8**(4), S87–S93 (2006).

1. Introduction

Coherent fluctuations or collective oscillations of mobile electrons, called surface plasmon polaritons (SPP), are generated at the interface of two media having relative permittivity with opposite signs (e.g. the metal-dielectric interface) when excited by light. These surface plasmon polaritons or waves are transverse magnetic (TM) polarized electromagnetic waves propagating parallel to the interface of the two media [1–3] and are highly sensitive to the refractive indices of the media involved—the refractive indices of the metal (metallic thin film or nanostructures) as well as of the dielectric media next to the metallic surface. In most surface plasmon resonance sensors, coupling of the incident radiation into surface plasmons is achieved either by using a glass prism (Kretschmann or Otto configurations [4, 5]), a grating or waveguide, which includes optical fiber waveguides [6–8]. Coupling of the incident radiation to SPPs in nanohole arrays has also been previously described [9–11]. In the past decade, the surface-sensitive optical phenomenon of surface plasmon resonance (SPR) and surface plasmon resonance imaging (SPRI) have emerged as promising techniques for chemical sensing and detection of real-time, label-free detection of biomolecular interactions on the surface of the metallic media.

The plasmon imaging reading systems used in SPRI allow easy access to real-time monitoring of biochip interactions and changes of refractive indices, and do not require any labeling [12, 13]. In traditional interpretation of SPR sensing and imaging data, it is assumed that the adsorbed chemical and biological molecules form a continuous film on the surface of the metallic films (i.e. total coverage is assumed). This assumption leads to the prediction of monomodal propagation of plasmons on the surface of the metallic film corresponding to the relative permittivity of the media (molecular film) next to the metal, which results in a single dip in the reflection spectrum associated with the plasmon resonance excitation at a given angle (for a fixed wavelength of the excitation radiation) or wavelength (for a fixed angle of incidence of the excitation radiation). As the thickness of the adsorbed layer is increased, the single plasmon resonance-related dip in the reflection spectrum associated with the

#165623 - $15.00 USD Received 2 Apr 2012; revised 16 May 2012; accepted 14 Jun 2012; published 1 Oct 2012

monomodal propagation shifts to correspond to a change in refractive index of the overlap volume associated with the surface plasmon wave propagating on the metal-dielectric interface. Hence, a best guess of the effective refractive index of the medium in immediate vicinity of the metallic film (due to adsorption of the molecules on the surface of the film) as well as of the bulk refractive index of the medium surrounding the molecular layer is based on the position and relative shifts of the angular reflectance curves (or the spectral reflectance curves) as the thickness of the adsorbed molecules is increased.

In actual SPR and SPRI sensors, the biochips employed may have different dielectric structure domain sizes—ranging from a few nanometers to 100s of micrometers—of the chemical or biological assembled on the surface of the continuous as well as nano- or micro-structured thin metallic films employed for SPR sensing. As illustrated on Fig. 1, two different kinds of regions exist on the surface of the homogenous metallic films on which surface plasmons are propagating—those two regions have different dielectric characteristics—first the regions, labeled A, which are assumed to be characterized by "solvent only (taken as water in calculations in this paper)" and second the regions, labeled B, having the extra dielectric layer in the vicinity of the metallic film. One should note that adding an extra homogeneous layer of dielectric would not change the issue discussed therein. The different regions, A and B, have structures of different refractive indices, and should therefore have different angular or spectral conditions for the propagation of plasmons. As they support different modes of surface plasmon propagation, they have different associated coupling resonances.

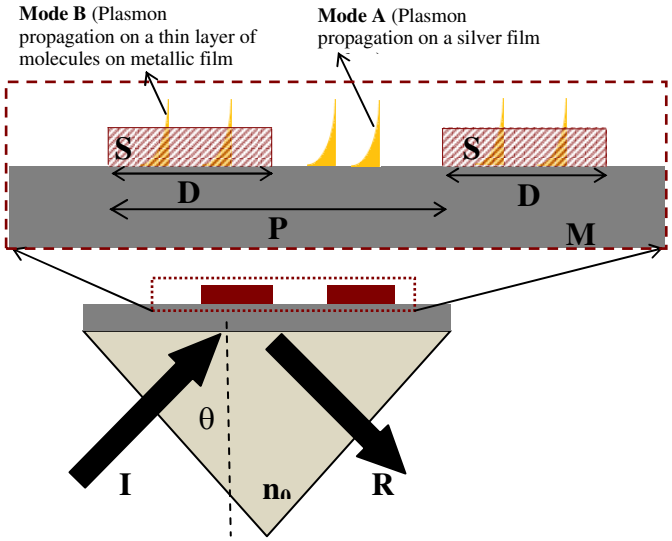

Fig. 1. Schematic showing Kretschmann configuration employed for coupling of incident radiation to surface plasmons on the surface of a plasmonic thin film on which molecules form periodic domains on the surface of the metallic film. The incident and reflected radiation are indicated by symbols **'I'** and '**R'**, respectively. While **'M'** indicates a plasmonic film such as a silver film, **'S'** indicates a thin layer of molecules on the surface of the metallic film. **'P'** shown in the above figure indicates the periodicity of the nano- or micro- structured molecular domain or the periodic "domain size" and **'D'** indicates the size of the nano- or micro- structured domain that is occupied by the molecules. Fraction (**'f'**) of nano- or micro- structured domain occupied by molecules is given by **'f' = (D)/(P)**.

As illustrated in Fig. 2, to add an extra layer of the dielectric, i.e. going from the case "100% of A" to the case "100% of B"—as it happens when binding a total coverage of target material—one can suggest two pathways. The classical pathway, which is generally assumed in most published data concerning propagative plasmonic sensing, is the one based on the assumption of a homogeneous layer of higher index material, for which either the thickness or the effective optical index is increased while the other quantity is assumed to be constant –

#165623 - $15.00 USD Received 2 Apr 2012; revised 16 May 2012; accepted 14 Jun 2012; published 1 Oct 2012

such interpretation clearly leads to a monomodal transition (labeled MMT) with a unique reflectivity dip translating from mode A to mode B. The other pathway that should also be considered consists of laterally adding a block of extra-dielectric, as if paving the metal surface. Clearly if those blocks have lateral dimensions large as compared to the plasmon propagation lengths, the dip associated with mode A will gradually disappear as the dip associated to mode B will rise, with an isobestic point where both modes happen to have same reflectivity. Such bimodal transition pathway is labeled BMT. However if the lateral sizes of such blocks are small and neglectable, effective dielectric refractive index behavior will be observed and the A to B transition will merge with the case of MMT.

Studying such transition from clear BMT behavior to clear MMT behavior is the object of this communication. It will be illustrated later by the results of this study that in the case of a small domain size, only a single mode of propagation (monomodal propagation) exists as indicated by only one dip in the angular reflectance curves associated with metallic film having a periodically structured array of molecules on its surface. As the domain size is increased, there is a transition from the monomodal propagation to the existence of two distinct modes of propagation (called bimodal propagation) as indicated by the existence of two dips in the angular reflectance curves associated with metallic film having a periodically structured array of molecules (See Fig. 2 (a)). Hence, one of the objectives of this work is to evaluate the transition point from monomodal to bimodal propagation—i.e. the size of the domain above which the propagation of two modes exists in a structured array of molecules on the surface of a metallic thin film. A monomodal to bimodal reflectance curve evolution (for both angular and wavelength reflectance curve) also occurs when for a given size of the domain, the fraction (f) of the molecules occupying each domain is varied from 0 to 1.

It is interesting to note that in SPR sensing and SPRI, the target materials have a given thickness and assemble more like blocks on the surface of the metallic films, which is functionalized with a receptor or probe molecules. As the adsorbed molecules are deposited in a non-continuous manner on the surface of the metallic films, there are domains of these molecules on the plasmonic films. Moreover, controllable development of nano- and micro-structured domains of molecules on the surface of a continuous metallic film [14, 15] are also being investigated. As SPR sensing and imaging are becoming more and more widespread, it is becoming increasingly important to understand the nature of plasmon propagation (monomodal or bimodal propagation) on the surface of metallic films so as to accurately interpret the sensing and imaging experimental results. Along with data interpretation, it is also important to estimate the size of the domains as well as the thickness of the molecules adsorbed on the surface of the metallic films on which the surface plasmons are propagating. The results of this study could enable theoretical estimation of the domain size and thickness of the molecules adsorbed on the surface of metallic films by observing the angular reflectance curves obtained from the metallic films and fitting the reflection data to that theoretically obtained for monomodal or bimodal plasmon propagation in nanostructured domains of molecules on the surface of metallic films. It has to be noted that in real samples, the dispersion in domain size could lead to a broadening of the multimodal behavior different from the purely monomodal one. Moreover, it could enable predicting angular reflectance curves of a metallic film on which adsorbed molecules form domains—if the size of the domains and the thickness of the adsorbed films are known.

In spectroscopy, an isobestic point is a specific wavelength at which two chemical species or group of species exhibit the same spectroscopic properties (e.g., molar absorptivity), which results in the overall absorption of the mixture of two chemicals being independent of the ratio of the two (or group of) chemical species in the mixture, but is only

#165623 - $15.00 USD Received 2 Apr 2012; revised 16 May 2012; accepted 14 Jun 2012; published 1 Oct 2012

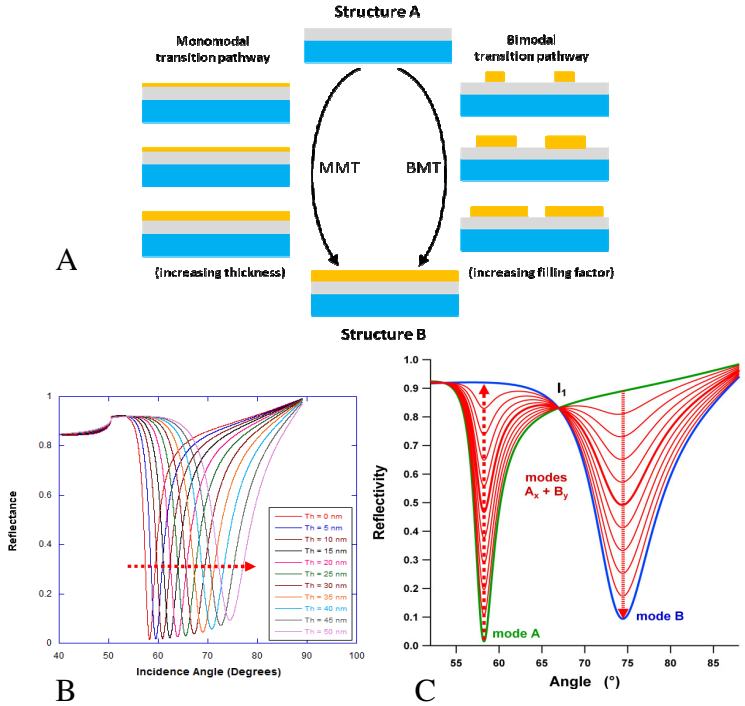

Fig. 2. (A) A schematic showing monomodal transition (MMT)—on increasing the thickness of continuous molecular layers on plasmonic thin films—as compared with a biomodal transition (BMT) that occurs when the molecular layer forms periodic domains and the size of the domains or the filling factor (for a given domain size) is increased. (B) Classical case of mode shift, i.e. the MMT case, as the thickness (Th) of the molecular film grows from 0 nm to 50 nm, i.e. from 0% to 100% (in intervals of 10%) of the maximum thickness (Thmax = 50 nm). The RCWA calculated reflectance spectra were obtained for a silver film with thickness (Th_{Ag}) of 50 nm deposited on SF11 glass (n_{SF11} = 1.723), the refractive index (RI) of the medium ($n_{molecule}$) above the silver film being 1.58 (mode B only, where molecules are present). (C) Schematic of reflectance spectra when molecular layer forms periodic domains on the plasmonic thin film such that two distinct surface plasmon propagation modes exist—mode A in regions where there are no molecules and mode B in regions where the molecules are present. This figure shows the schematic of reflection spectra when % of mode A is decreased and % mode B is increased (in intervals of 10%)—exhibiting one isobestic point I_1—obtained by proportionately mixing reflectance spectra obtained using RCWA calculations from a silver film either completely covered by molecules (mode B only) or completely covered by surrounding media having a RI ($n_{solvent}$) of 1.33 (mode A only). The incident wavelength ($\lambda_{incident}$) in the calculations is 550 nm.

related to their total concentration. In this paper, we extend the isobestic concept and use the term 'isobestic point' to designate that invariant point—either an angle of the incidence (for a fixed radiation wavelength) or a wavelength (for a fixed angle of incidence)—at which the reflectivity from a plasmonic thin film remains the same irrespective of the domain size of the molecules adsorbed on the surface of the plasmonic thin film, especially as the domain size goes from sub-5 nm range to above 100 microns in size. The numerical calculations described in this paper enable us to estimate the isobestic point or points—the angles of incidence (for a fixed radiation wavelength) or a wavelength (for a fixed angle)—at which the reflectance (or reflectivity) remain constant as the size of the domain of molecules adsorbed on the metallic film on which the surface plasmons are propagating is varied from sub-10 nm regime to 100s of microns in dimension. This isobestic behavior is also observed as we change the ratio of the domain itself i.e. on varying the value of 'f' from 0 to 1.

We carried out calculations on different types of plasmonic films (in particular gold and silver thin films), and at different wavelengths varying from 500 nm to 800 nm. In this paper,

#165623 - $15.00 USD Received 2 Apr 2012; revised 16 May 2012; accepted 14 Jun 2012; published 1 Oct 2012

we will illustrate our point with angular reflectivity data using silver at 550 nm, 600 nm, and 700 nm because we can clearly illustrate the transition from monomodal to bimodal propagation as well as the isobestic behavior when the size of the domain as well as the fraction 'f' of the molecules occupying each domain (for a given size of the domain) are varied. Such angular reflectivity representation was preferred in this paper over spectral representation as we did not want to discuss the impact of the dispersion relations, which would have added discussion subtleties without any extra value. We also employed analytical calculations—using the Rouard extended method [16]—to determine the angular reflectivities from metallic films having homogenous dielectrics i.e. either region A entirely on the surface of the metallic films (f_A = 100%) or region B entirely on the surface of the metallic films (f_A = 0% and f_B = 100%). These calculations using the Rouard method were carried out to double-check the results from the RCWA calculations, for these two sets of cases, and were found to match the results from the RCWA calculations.

2. Numerical simulations based on rigorous coupled wave analysis (RCWA)

2-D Rigorous Coupled Wave Analysis (RCWA) calculations [17] of angular reflectance curves from the metallic film having different periodically structured domains of molecules (higher refractive index regions) were carried out using a software called DiffractMOD 3.1, which allows a full vectorial solution of the Maxwell's equations in the Fourier domain, wherein periodic permittivity functions are represented using Fourier harmonics and the electromagnetic fields are represented as summations over coupled waves. RCWA analysis significantly decreases computational time and required memory size as compared to the FDTD method and was therefore employed to calculate the wavelength and angular dependence of the reflectance of such a dielectric grating on silver. The RCWA calculations carried out in this paper employed an extended Debye model to describe the dispersion relation of relative permittivity of silver and gold [18]. We have previously employed RCWA calculations for studying the plasmonic behavior of gold nano-lines employed for SPRI [19] as well as narrow-grove metallic nano-gratings employed for SPR sensing [20]. In the RCWA calculations carried out for metallic films having different periodically structured domains of molecules, TM polarized plane waves (at different wavelengths and angles of incidence) were incident on the metallic film (having different periodically structured domains of molecules) and the reflectance calculated as a function of the incident angle or wavelength. In the simulations, the thickness of the silver films was taken to be 50 nm—the silver films being deposited on a 1 nm thick chromium adhesion layer which is deposited on SF11 glass substrates having refractive index (RI) of ~1.723. Simulations were performed to cover the angular range of 40-90°, the incident radiation wavelength range of 450-900 nm. The angle of incidence here refers to the angle made by the incident radiation with the normal to the metallic thin film. The RCWA calculations were carried out to determine the effect of varying the domain size of molecules covering a plasmonic film (silver thin film)—as well as the fraction of the molecules covering each domain (for a given domain size)—with the localized refractive index of the molecular layer being taken as 1.58, and of the refractive index of the bulk media surrounding the plasmonic films and the molecules taken as 1.33. In order to clearly illustrate the isobestic behavior as well as the monomodal to bimodal transition, we carried out the angular reflectivity (varying angle of incidence from 40° to 90°) calculations at a fixed wavelengths (550 nm, 600 nm, and 700 nm). In all the RCWA calculations carried out for domain sizes less than or equal to 5 microns, 5 Fourier harmonics were employed as this number of harmonics was found to be sufficient for convergence. For a 10 micron domain size, 10 Fourier harmonics were found to be sufficient for convergence. For domain sizes larger than 10 microns (50, 100, and 500 microns), 50 Fourier harmonics were employed as that provided convergence.

In the RCWA calculations carried out in this paper, we employed a Kretschmann configuration (See Fig. 1) for coupling of the incident radiation to surface plasmons on the surface of a plasmonic thin film (silver thin film) on which molecules form periodic domains on the surface of the metallic film. In this work, we increase ‘f’ and observe the transition of

#165623 - $15.00 USD Received 2 Apr 2012; revised 16 May 2012; accepted 14 Jun 2012; published 1 Oct 2012

the surface plasmon propagation from monomodal to bimodal above certain domain sizes 'D' (or periodicities, as D = P*f). Moreover, we also increase the domain sizes of the periodic domains (for one-dimensional periodic arrangement of molecular domains on the surface of metallic films, on whose surface the surface plasmon wave propagates) and observe the transition of the surface plasmon propagation from monomodal to bimodal, for a given fraction of the nano- or micro- structured domain that is occupied by the molecules.

3. Results and discussions

RCWA calculations highlighting the classical case of single mode shift — as the thickness (Th) of the molecular film grows from 0 nm to 50 nm, i.e. from 0% to 100% (in intervals of 10%) of the maximum thickness (Th_{max} = 50 nm)—are shown in Fig. 2 (b). In the convention employed in this paper, mode A_xB_y (x + y = 1), describes monomodal behavior where the net curve is the product of modes A and B, whereas the mode $A_x + B_y$ define the bimodal behavior taking the average of modes A and B. Hence, in these calculations only the mode B (see Fig. 1) of the propagating surface plasmons is present in the region above the metallic film containing the molecular films of different thicknesses. In classical interpretation of SPR sensing and imaging data, total coverage of the adsorbed chemical and biological molecules is assumed. This leads to the prediction of monomodal propagation of plasmons on the surface of the metallic film corresponding to the relative permittivity of the media next to the metal, which results in a single dip in the reflection spectrum associated with the plasmon resonance excitation at a given angle (for a fixed wavelength of excitation radiation) or wavelength (for a fixed angle of incidence). As the thickness of the adsorbed layer is increased, the single plasmon resonance related dip in the reflection spectrum associated with the monomodal propagation shifts—Fig. 2 (b) shows a right shift in the angular reflectance curves for a fixed wavelength (550 nm) of an incident radiation—to correspond to a change in refractive index of the overlap volume associated with the surface plasmon wave propagating on the metal-dielectric interface.

Employing the classical SPR interpretation based on the assumption of total coverage, one can approximate the thickness of the molecular film adsorbed on the surface of the plasmonic thin film based on the calculations shown in Fig. 2 (b) (based on position and relative shifts of the angular reflectance curves as thickness of the adsorbed molecules is increased) if the effective refractive index of the medium in immediate vicinity of the metallic film as well as the bulk refractive index of the medium surrounding the molecular layer are known. Similarly, one can also approximate the RI of the molecular layer if its thickness is known.

It is known in SPR imaging and sensing that the chemical or biological molecules adsorbed or deposited on the surface of the metallic films, do not have total coverage and rather deposit in steps which leads to the formation of periodic domains of these molecules with the domain sizes ranging from a few nanometers to 100s of micrometers. Two different kinds of regions exist on the surface of the homogenous metallic films on which surface plasmons are propagating—first the regions (say region B) having molecules probe and target molecules and second the regions having only water (say region A) in the vicinity of the metallic film (See Fig. 1). As these different regions have different refractive indices and should therefore have different angular or spectral conditions for the propagation of plasmons, they should theoretically support different modes—say mode A in region A and mode B in region B—of surface plasmon propagation and the net angular reflectance curves should be a mixture of mode A and mode B depending on the proportion of the two regions i.e. fraction of the total domain period that is occupied by the molecules (f_B) or not occupied by molecules ($f_B = 1 - f_A$). Figure 2 (c) (for 550 nm wavelength of the incident radiation) shows theoretical angular reflectance curves obtained by mixing the RCWA calculated angular reflectance curves for the cases where there is region A only (green curve) above the metallic film propagation the surface plasmons or only region B (blue curve). The red curves in Fig. 2 (c) show the theoretically calculated angular reflectance curves obtained by proportionately mixing reflectance angular reflectance curves obtained using RCWA calculations from a silver film either completely covered by molecules (mode B only) or completely covered by

#165623 - $15.00 USD Received 2 Apr 2012; revised 16 May 2012; accepted 14 Jun 2012; published 1 Oct 2012

surrounding media with n = 1.33 (mode A only). In Fig. 2 (c), one can observe one isobestic point (point I_1) in this figure, which indicates the point at which the reflectance remains constant irrespective of the proportion of the mode A or mode B that is propagating (i.e. irrespective of the fraction of the periodic domain covered with molecules or of the angle of incidence of the radiation.

Figure 3 shows RCWA calculations of angular reflectance curves as the proportion of each periodic domain occupied by molecules i.e. f_B is increased from 0% to 100% (in intervals of 10%) for different periodicities ranging from 0.05 µm to 100 µm. It is observed from Fig. 3 (a) that when the domain size is small, the periodicity being 0.05 µm, there is only one dip in the angular reflectance curves indicating the existence of only one mode, i.e. monomodal propagation of surface plasmons. It is also interesting to note from Fig. 3 (a) that as the proportion of each periodic domain occupied by molecules i.e. f_B is increased from 0% to 100%—with the thickness of the molecular film remaining constant i.e. 50 nm—the

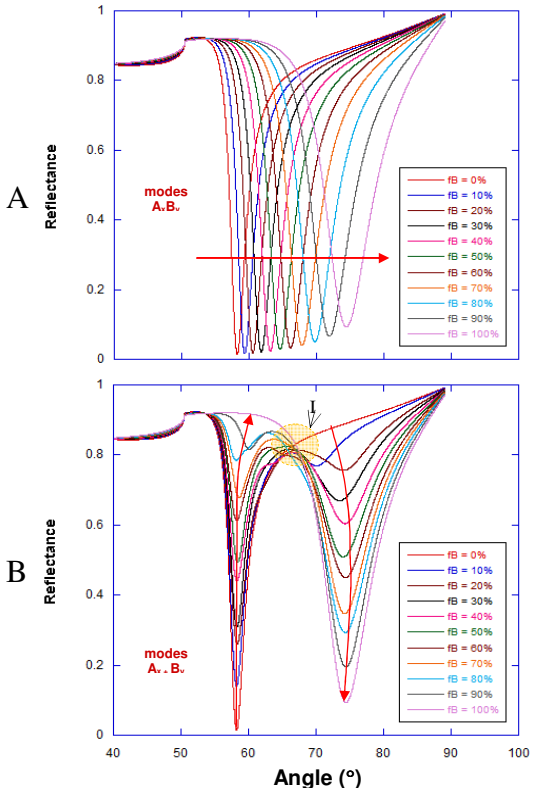

Fig. 3. RCWA calculations showing reflectance spectra as the proportion of each periodic domain occupied by molecules i.e. f_B is increased from 0% to 100% (in intervals of 10%) for different periodicities: (a) 50 nm and (b) 100 µm. Values of $\lambda_{incident}$, 'Th', $n_{solvent}$, $n_{molecule}$, and n_{SF11} were taken the same as in Fig. 2.

angular reflectance curves exhibit a right shift. In the case of a larger domain size, the periodicity being 100 µm (Fig. 3(b)), we observe the appearance of two dips in the angular reflectance curves (indicating the existence of two modes, i.e. bimodal propagation of surface plasmons) when the proportion of each periodic domain occupied by molecules i.e. f_B is increased from 0% (only one mode, i.e. mode A, exists when f_B = 0%, shown by the red curves in Fig. 3(b)) till the value of f_B reaches 100% when again only one mode, i.e. mode B, exists shown by the light purple curve in Fig. 3 (b). Moreover, in Fig. 3 (b), one can observe an isobestic point 'I_1' which is not as distinctly a single point as the theoretically generated

#165623 - $15.00 USD Received 2 Apr 2012; revised 16 May 2012; accepted 14 Jun 2012; published 1 Oct 2012

curve shown in Fig. 2 (c) but still highlights that the transition from 'monomodal to bimodal' and then from 'bimodal to monomodal'—on increase of the proportion of each periodic domain occupied by molecules i.e. f_B from 0% to 100%—is for most part isobestic in nature; and there is a very small region (almost tending to a point 'I') that represents the reflectance as the proportion of each periodic domain occupied by molecules (f_B) is varied.

Figure 4 (a) shows theoretically generated reflectance spectra (for the case when f_B = 50%) obtained by proportionately mixing (fitting) monomodal and bimodal angular reflectance curves—i.e. angular reflectance curves obtained using RCWA calculations for silver film having f_B = 50% and periodicity either being very small i.e. 20 nm (such that monomodal behavior is exhibited, as shown by the dark golden curve) or very large i.e. 1000 microns (such that bimodal behavior is exhibited, as shown by the dark purple curve). Figure 4 also shows the RCWA calculated angular reflectance curves for the cases where there is region A only (green curve) above the metallic film or only region B (blue curve). The red curves in Fig. 4 show the theoretically calculated angular reflectance curves as the % of monomodal behavior is decreased and % bimodal behavior is increased obtained by proportionately mixing completely monomodal (the periodicity being less than 100 nm) and completely bimodal (the periodicity being greater than 500 µm) angular reflectance curves that are calculated using RCWA.

In the curves obtained by proportionately mixing the monomodal and bimodal behavior in Fig. 4, one can observe the existence of two isobestic points (points I_2 and I_3) which are the points at which the reflectance remains constant irrespective of the proportion of the monomodal or bimodal behavior that exists in the propagating surface plasmon waves. Hence, the theoretical calculations described in this paper enable us to estimate the isobestic point as the domain size of molecules adsorbed on the metallic film on which the surface plasmons are propagating is varied. We observe in Fig. 4 (b) that the curve C_2 calculated

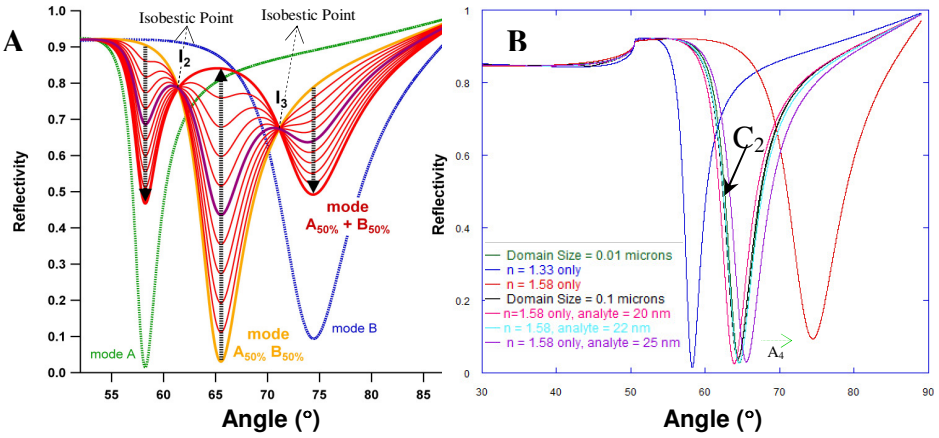

Fig. 4. (A) Theoretically generated reflectance spectra that represent a mixture of bimodal and monomodal behavior for f_B = 50%, clearly showing two isobestic Points I_2 and I_3. The spectra were obtained by proportionately mixing spectra obtained using RCWA calculations for silver film having f_B = 50% and periodicity either being very small i.e. 20 nm (such that complete monomodal behavior is exhibited) or very large i.e. 1000 microns (such that complete bimodal behavior is exhibited). Values of $\lambda_{incident}$, 'Th', $n_{solvent}$, $n_{molecule}$, and n_{SF11} were taken the same as in Fig. 2.(B) RCWA calculations showing reflectance spectra obtained from a silver film—covered with periodic domains of molecules (f_B = 50%), domain size being 10 nm and the thickness of the molecular film being 50 nm—as compared with spectra from silver films coated with a continuous layer of molecules (i.e. full coverage) having different molecule thicknesses., $\lambda_{incident}$ being 550 nm.

using RCWA (for the thickness of the molecular layer being 50 nm and f_B = 50%) when the domain periodicity is very small (20 nm or 200 nm) exhibits completely monomodal behavior and has only one peak in the reflection spectrum. Arrow A4 in Fig. 4 (b) shows the right shift

#165623 - $15.00 USD Received 2 Apr 2012; revised 16 May 2012; accepted 14 Jun 2012; published 1 Oct 2012

of the angular reflectance curve when the thickness of a continuous molecular thin film is increased from 0 nm (blue) to 50 nm (red)—the intermediate values being 20 nm (pink), 22 nm (light blue), and 25 nm (purple). The reflection spectrum, including the spectral position of the dip, of C_2 (in black dashed line) overlaps with the reflectance spectrum obtained from a silver thin film having a continuous molecular layer (for full coverage of molecules) having a thickness of ~22 nm.

Figure 5 shows RCWA calculations of angular reflectance curves as the periodicity of the molecular domains is varied from 20 nm to 1000 μm, the proportion of each periodic domain occupied by molecules i.e. f_B being 50%. The wavelengths of the incident radiation in the RCWA calculations in Figs. 5 (a), 5 (b) and 5 (c) were taken as 550 nm, 600 nm, and 700 nm, respectively. It is observed from Fig. 5 (a) that when the domain size (domain periodicity/2) is small, the periodicities being 0.02 μm and even 2 μm, there is only one dip in the angular reflectance curves indicating the existence of only mode, i.e. monomodal propagation of surface plasmons. As the domain size is increased above 1.75 μm, one can observe the appearance of an angular reflectance curves having three dips (more clearly visible when the domain periodicity size is 2.5 μm in Fig. 5 (a))—the angular reflectance curves representing a true average of monomodal and bimodal behavior (as predicted theoretically by Fig. 4). As the size of the domains is further increased, the middle peak (shown by arrow A_2 decreases in size till it disappears for the larger domain sizes (for example periodicity being 200 μm and 1000 μm). On the other hand, the dips indicated by arrows A_1 and A_3 grow and become fully evolved, and for larger domain periodicities (e.g. 200 μm and 1000 μm) there are only two dips indicating a fully bimodal behavior.

Moreover, in Fig. 5 (a) (as well as in Figs. 5 (b) and 5 (c)), one can observe two isobestic points 'I_2' and 'I_3', as predicted by the theoretically generated curves shown in Fig. 4 (a). The isobestic points are not as distinctly single points as the theoretically generated curves shown in Fig. 4 (a) but still highlight isobestic transition from 'purely monomodal behavior' to a 'mixture of monomodal and bimodal' behavior, when the size of the molecular domains is increased above 1.75 μm. Subsequently, we also observe a transition from 'a mixture of bimodal and monomodal behavior' when the size of the domain is increased above 1.75 μm to 'purely bimodal behavior' when the size of the domain is increased above ~100 μm. Figures 5 (b) and 5 (c) (with the calculations carried out for 600 nm and 700 nm being the incident wavelengths) also show the isobestic region but the region is wider than that compared with calculations carried out for the incident wavelength of 550 nm. Moreover, we also observe that the transition from a 'purely monomodal behavior' to a f'mixture of monomodal and bimodal' behavior occurs for a domain periodicity which is higher for an incident wavelength of 700 nm as compared to the point for an incident wavelength of 550 nm. Similarly, we observe that the transition from a 'purely monomodal behavior' to a 'mixture of monomodal and bimodal' behavior occurs for a periodicity of the domain which is higher for an incident wavelength of 700 nm as compared to the point for an incident wavelength of 600 nm. Some extra dips in the reflectance spectra—other than those resulting from the pure A + B, pure AB modes, and a mixture of A + B and AB modes—result due to the periodic nature of the domains on top of the metallic films and the grating-effect resulting from these domains. Finally, Fig. 6 illustrates the transition from a 'purely monomodal behavior', MMT, AB, to a 'mixture of monomodal and bimodal' and then to a

#165623 - $15.00 USD Received 2 Apr 2012; revised 16 May 2012; accepted 14 Jun 2012; published 1 Oct 2012

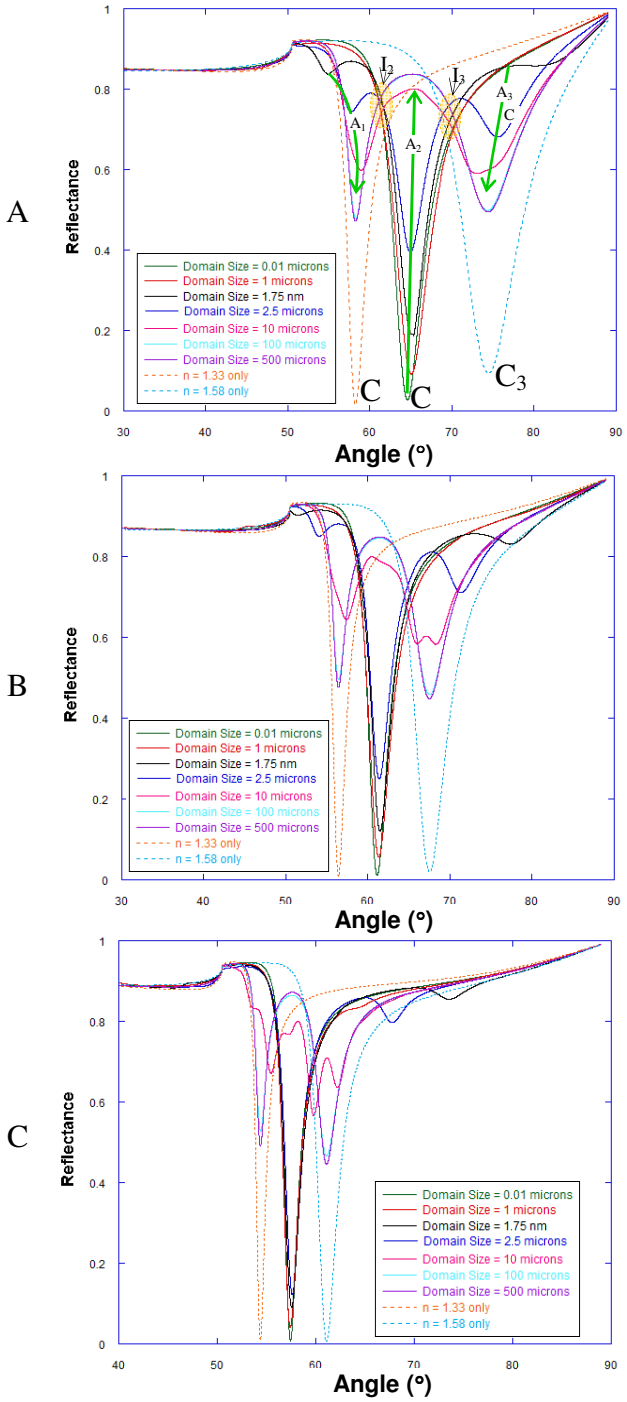

Fig. 5. RCWA calculations showing reflectance spectra obtained from a silver film covered with periodic domains of molecules (f_B = 50%) such that the periodicity of the domains was varied from 20 nm to 1000 μm. C_2 is the curve of the type 'AB' when 50% of the silver film is covered with the molecules for each domain size. I_2 and I_3 are the isobestic points. The values of 'Th', $n_{solvent}$, $n_{molecule}$, and n_{SF11} were taken the same as in Fig. 2. The incident wavelength in the calculations was (A) 550 nm, (B) 600 nm, and (C) 700 nm.

#165623 - $15.00 USD Received 2 Apr 2012; revised 16 May 2012; accepted 14 Jun 2012; published 1 Oct 2012

'purely bimodal behavior', BMT, A + B, as the periodicity of the domain is increased from ~20 nm to 100s of microns, for different wavelengths. Figure 6 shows data points for the extrapolated values of contents of the A + B mode and the complementary AB mode, as measured from their respected dips in the RCWA reflectance calculations, i.e. using normalized ratios of reflectivity at the AB peak (curve C_2 in Fig. 5a) normalized to 0 for minimum value and 1 for the highest obtained at the same angle for the average of A only and B only structures. Complementary data obtained using the A only and B only structure reflectivity angle peaks (C_1 and C_3 curves in Fig. 5a) were also calculated and smoothed checking that the sum of fraction $f_{AB} + f_{A+B}$ totaled 1. Such data normalization was carried out by employing the three different wavelengths of the incident radiation, 550 nm, 600 nm, and 700 nm. The dashed lines represent fits to a sigmoid transition function. The fitting parameter data for the different wavelengths of the incident light are respectively:

550 nm: Transition domain size – 2.7 μm, width of transition – 0.76 μm

600 nm: Transition domain size – 3.5 μm, width of transition – 1 μm

700 nm: Transition domain size – 5.6 μm, width of transition – 1.7 μm

The plot actually highlights that as the size of the domain is small (say far less than 1μm for 550 nm wavelength of incidence, as shown in Fig. 5 and Fig. 3), the reflectance curves represent a monomodal curve (curve C_2) with a single resonance dip located in the middle of those corresponding to only mode A (curve C_1 in Fig. 5 (a)) and only mode B (curve C_3 in Fig. 5 (a)). Such type of a plot being listed in Fig. 6 as the mode type 'AB' or 'AB' singular mode. As we move to very large values of the dielectric domain sizes (greater than 10 μm), we obtain curves that are proportionately summative averages of curves C_1 and C_3 in Fig. 5a, and these curves are listed in Fig. 6 as being the mode type '(A + B)/2' or just 'A + B' mode. When the dielectric domain sizes are greater than 1 micron but below 10 microns, hybrid curves such as the curve C_4 shown in Fig. 5a, are observed—these hybrid curves being proportionately summative averages of the 'AB' and 'A + B' modes.

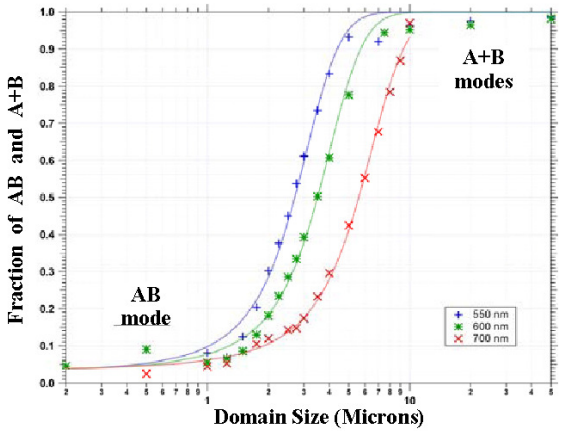

Fig. 6. Transition from "**AB**" to "**(A+ B)/2**" as a function of the domain size (half of periodicity). For domain sizes lying between ~1.5 μm to ~10 μm, intermediate behavior between the "**AB**" and the "**(A+ B)/2**" modes is observed. Here mode (**A**) corresponds to metallic film only while mode (**B**) corresponds to uniform layer of molecules on the surface of the metallic film. Mode "**AB**" here corresponds to monomodal behavior while mode "**(A+ B)/2**" corresponds to bimodal behavior.

In the case of a continuous silver thin film—having a refractive index 'n_s' = 1.58 of the medium next to the silver film—the surface plasmon propagation lengths (δ_{SPP}) [21] were calculated as 6.7 μm, 8.5 μm, and 12.9 μm, when the wavelengths of the incident light are 550 nm, 600 nm, and 700 nm, respectively. The surface plasmon wavelengths (λ_{SPP}) [21] in this case are 321.6 nm, 354.8 nm, and 420.8 nm when the wavelengths of the incident light

#165623 - $15.00 USD Received 2 Apr 2012; revised 16 May 2012; accepted 14 Jun 2012; published 1 Oct 2012

are 550 nm, 600 nm, and 700 nm, respectively. Similarly, for a continuous silver thin film—having a refractive index 'n_s' = 1.33 of the medium next to the silver film—the surface plasmon propagation lengths (δ_{SPP}) were calculated as 12.1 μm, 15.2 μm, and 22.7 μm, when the wavelengths of the incident light are 550 nm, 600 nm, and 700 nm, respectively. The surface plasmon wavelengths (λ_{SPP}) in this case are 391.5 nm, 430.4 nm, and 507.7 nm when the wavelengths of the incident light are 550 nm, 600 nm, and 700 nm, respectively. We employed the dispersion relation for surface plasmon propagation on a metal-dielectric interface for the calculation of the plasmon resonance wavelength (λ_{SPP}) and the plasmon propagation length (δ_{SPP}) [21].

Figures 5 and 6 also shows that the domain size—at which the transition occurs from the 'AB' mode to 'A + B' mode—is higher for higher wavelength of the incident radiation (700 nm) as compared with 600 nm and 550 nm. This can be explained by the fact that the surface plasmon propagation length is larger for a larger wavelength of the incident radiation. For example, the transition occurs for 550 nm wavelength at ~2.7 microns domain size (domain periodicity being 5.4 microns). At 550 nm of the incident light, the surface plasmon propagation length (δ_{SPP}) is 6.7 μm, for a continuous silver film having a molecular thin film with a refractive index of 'n_s' = 1.58 adjacent to the silver film. As the wavelengths of the incident light are increased to 600 nm and 700 nm, the transition domain sizes increase to 3.5 microns and 5.6 microns, respectively. This is in accordance with the surface plasmon propagation length (δ_{SPP})—for a continuous silver film having a molecular thin film with a refractive index of 'n_s' = 1.58 adjacent to the silver film—increasing to 8.5 μm and 12.9 μm when the wavelengths of the incident light are increased to 600 nm and 700 nm, respectively. As shown in Fig. 6, we are able to obtain the transition point—in terms of the periodicity of the molecular domains—from a purely monomodal behavior of surface plasmon propagation to a mixture of bimodal and monomodal propagation, which can enable one to view experimental angular reflectance data and correctly interpret the experimental data to estimate the periodicity and size of the molecular domain. This can also enable more precise interpretation of the plasmonic biochip data when the domain sizes vary from hundreds of microns to sub-micron dimensions.

4. Conclusion

In this paper, RCWA numerical calculations were employed to study the propagation of surface plasmons in metallic films having periodic domains of chemical or biological molecules deposited on their surface. The calculations showed that when the size of the molecular domains (formed on top of the plasmonic thin films) is small (< 100 nm), a monomodal surface plasmon propagation behavior exists as indicated by only one dip in the angular reflectance curves. As the size of the molecular domains formed on the plasmonic thin films is increased, there is a transition from 'monomodal propagation behavior' to the existence of a 'mixture of monomodal and bimodal propagation behavior' which changes to a purely 'bimodal behavior' after the size of the domain periodicity is increased beyond ~10 micron. Moreover a transition from a monomodal behavior to bimodal behavior was observed when fraction of the molecules covering a given periodic domain surface is increased for larger domain sizes. The results of this paper can enable to not only correctly interpret the experimental angular or spectral reflectance data but also to predict domain size of the molecular domains above which a purely monomodal plasmon propagation transitions to a mixture of bimodal and monomodal propagation. The results of this paper also show that the transitions on changing the fraction or size of the domains exhibit isobestic behavior.

Acknowledgments

The authors would like to thank the sponsors of this work—National Institutes of Health, USA (Grants R01 EB006201 and R01 ES014774), the Indian Institute of Technology-Delhi, India and CNRS, France. Institut d'Optique is part of the European Network of Excellence Photonics4Life, P4L, granted by the FP7 framework. Dr. Canva also acknowledges partial financial support from the French DGA for his overseas sabbatical at Duke University.